Developing drag models for non-spherical particles through machine learning

Rui Ni, Gretar Tryggvason, Jiacai Lu, Xu Xu

JOHNS HOPKINS

Department of Mechanical Engineering
Johns Hopkins University

NATIONAL ENERGY TECHNOLOGY LABORATORY

Acknowledgement: Department of Energy, Office of Fossil Energy, Grant13034068 (PM: Omer R. Bakshi)

Oak Ridge Institute for Science and Education (ORISE)

William A. Rogers, Cheng Li, Xiongjun Wu, Avinash Vaidheeswaran, Mehrdad Shahnam, Jordan Musser, Jeff Dietiker, and many others in the Multiphase Flow Science group at NETL

Motivation: coal and biomass gasification

- Thermal conversion systems are very challenging to model:
  - Particles have complex shapes, a broad range of sizes, shapes and density.
  - Non-spherical particle interact with other particles.
  - Force closures are needed for non-spherical particles, i.e. drag and lift (maybe even other unsteady forces such as added mass and history force)

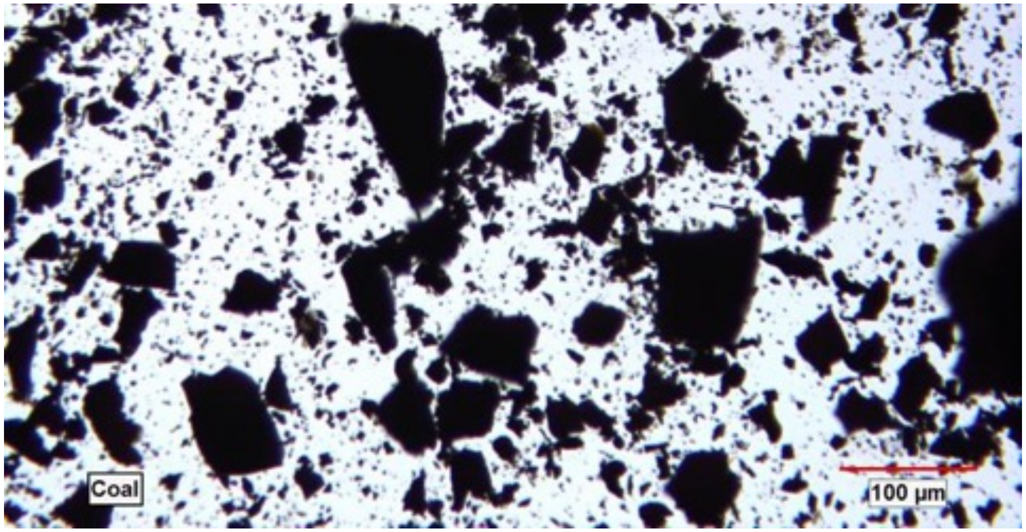

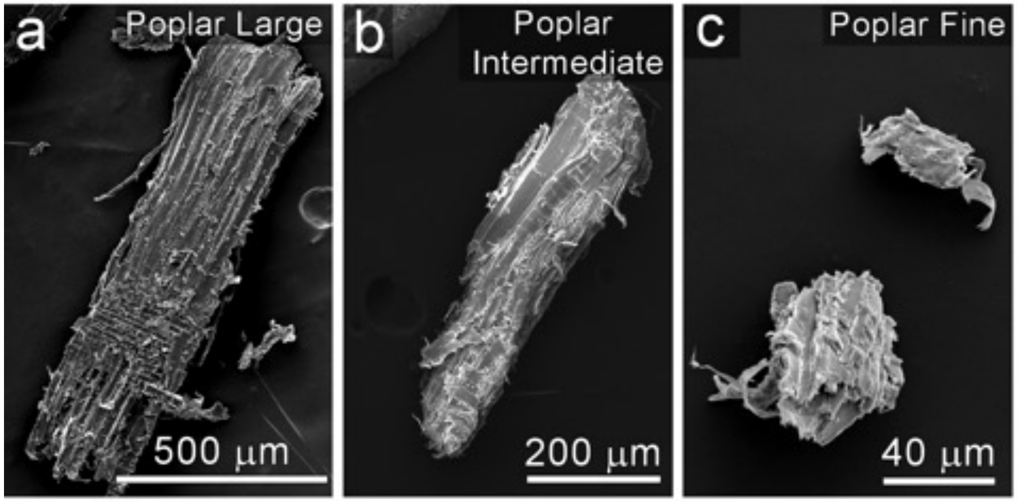

Objective: develop validated drag models for non-spherical particles

Drag Coefficient on Single Spherical and Non-Spherical Particle

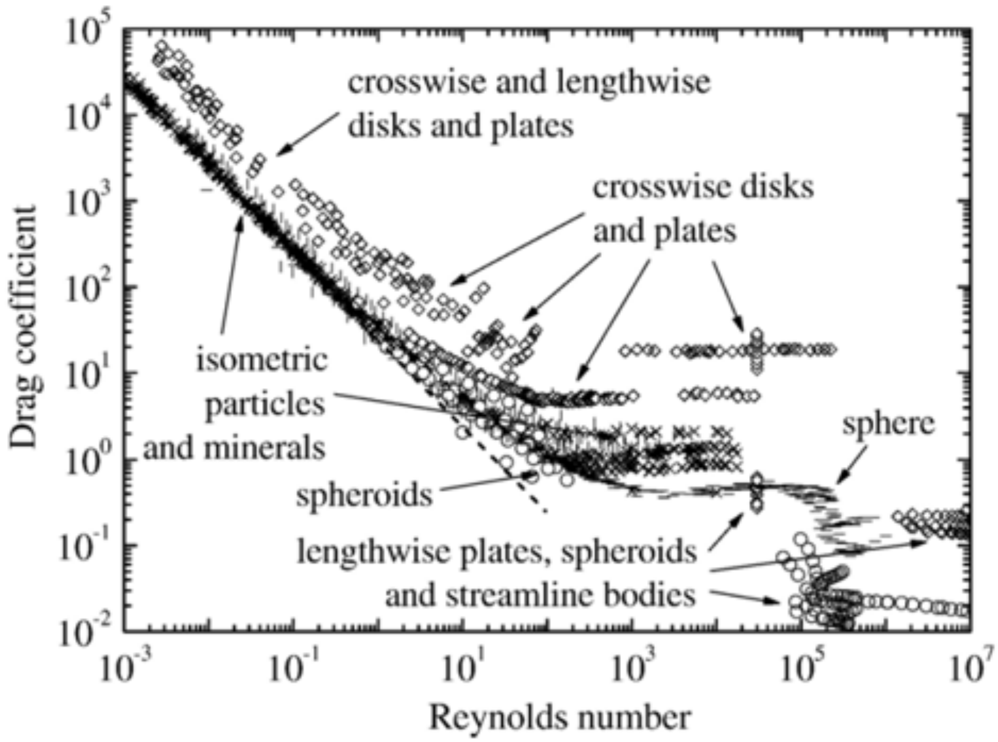

A. Hölzer, M. Sommerfeld / Powder Technology 184 (2008) 361–365

Sphere (Stokes flow): $c_D = \frac{24}{Re}$

Non-spherical particle (Stokes flow):

$$c_D = \frac{8}{\mathrm{Re}}\frac{1}{\sqrt{\Phi_\perp}} + \frac{16}{\mathrm{Re}}\frac{1}{\sqrt{\Phi}}$$

D. Leith, Aerosol Sci. Tech. 6 (1987) 153

Non-spherical particle ($Re < 10^5$):

$$\frac{c_d}{K_2} = \frac{24}{\mathrm{Re}K_1 K_2}\left(1 + 0.1118(\mathrm{Re}K_1 K_2)^{0.0567}\right) + \frac{0.4305}{1 + \frac{3305}{\mathrm{Re}K_1 K_2}}$$

$$K_2 = 10^{1.8148(-\log\phi)^{0.5743}}$$ (Newton factor)

G. H. Ganser, Powder Technol. 77 (1993) 143

Non-spherical particle ($Re < 10^5$):

$$c_D = \frac{8}{\mathrm{Re}}\frac{1}{\sqrt{\Phi_\parallel}} + \frac{16}{\mathrm{Re}}\frac{1}{\sqrt{\Phi}} + \frac{3}{\sqrt{\mathrm{Re}}}\frac{1}{\Phi^{\frac{3}{4}}} + 0.42 10^{0.4(-\log\Phi)^{0.2}}\frac{1}{\Phi_\perp}$$

Drag Coefficient on Packed Spherical Particle

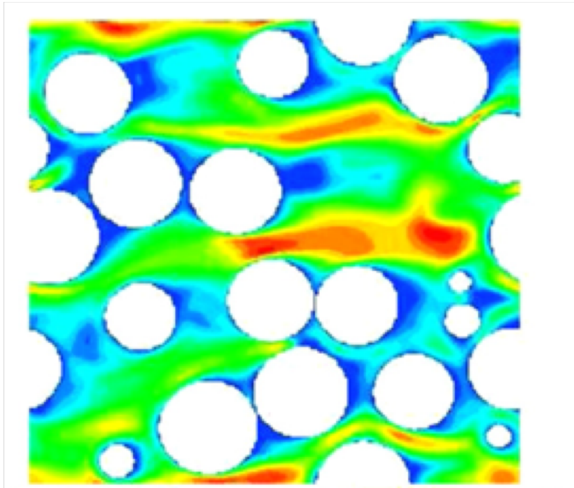

Tenneti et al. (2011)

$$F(\phi, \mathrm{Re}_m) = \frac{F_{\mathrm{isol}}(\mathrm{Re}_m)}{(1-\phi)^3} + F_\phi(\phi) + F_{\phi,Re_m}(\phi, \mathrm{Re}_m)$$

$$F_\phi(\phi) = \frac{5.81\phi}{(1-\phi)^3} + 0.48\frac{\phi^{1/3}}{(1-\phi)^4}$$

$$F_{\phi,\mathrm{Re}_m}(\phi, \mathrm{Re}_m) = \phi^3\,\mathrm{Re}_m\left(0.95 + \frac{0.61\phi^3}{(1-\phi)^2}\right).$$

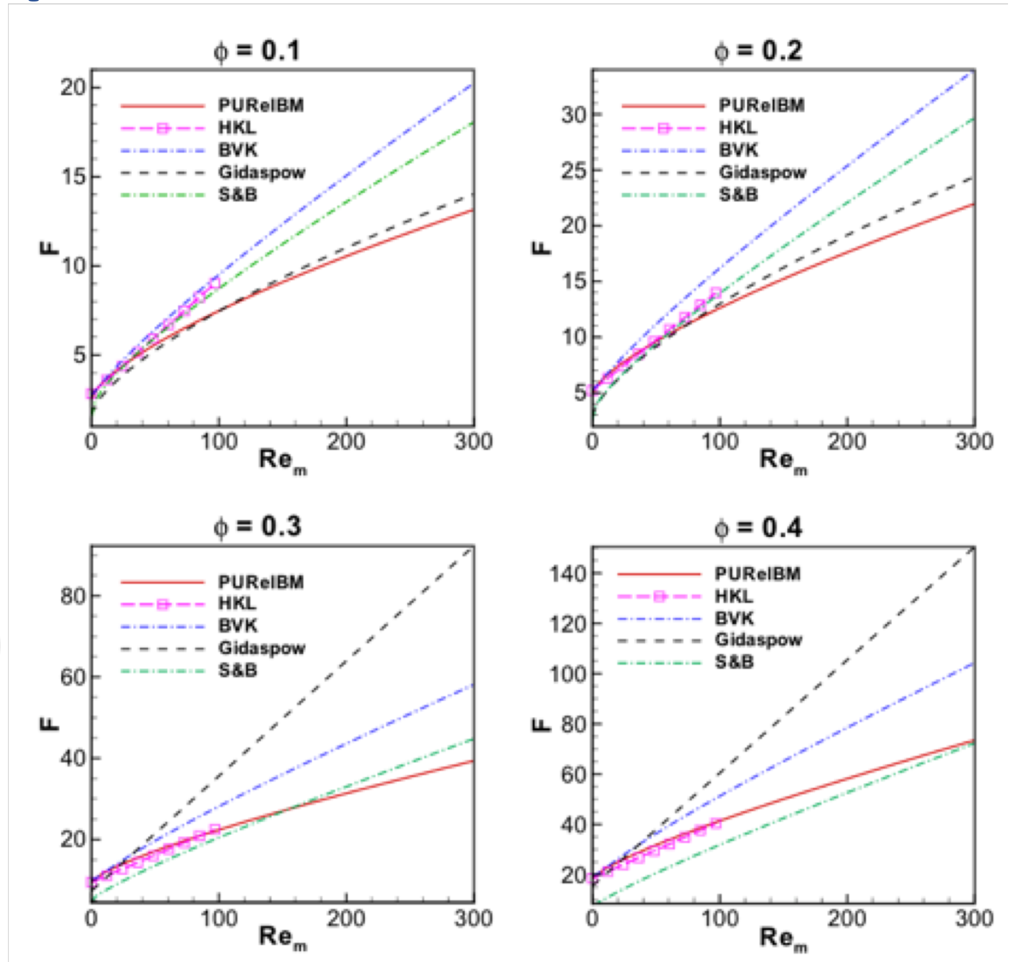

Tenneti et al. (2011);
Hill et al. (2001);
Beetstra et al. (2007);
Gidaspow (1986);
Syamlal and O'Brien (1987);

Tenneti et al. (2011)

Wen & Yu (1966) for dilute suspensions and Ergun's equation (Ergun 1952) for denser systems are the earliest experimental efforts.

Drag Coefficient on Packed Non-spherical Particle

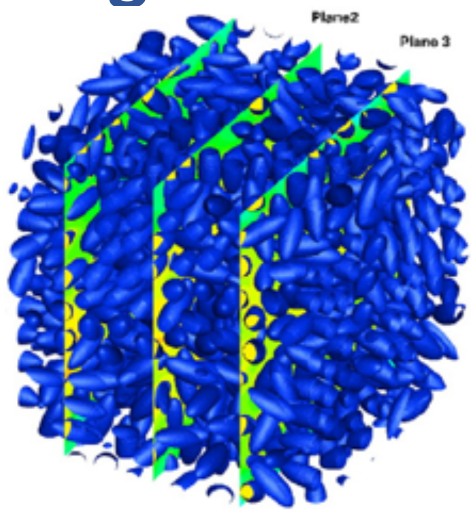

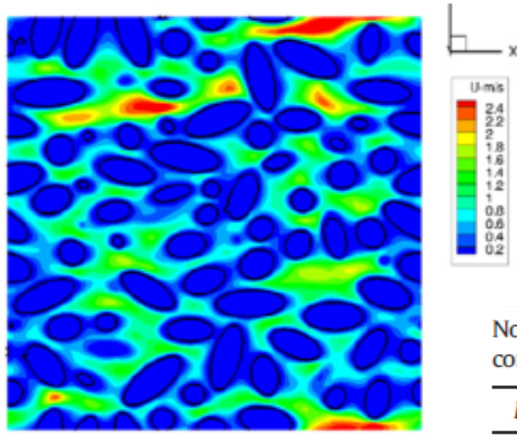

L. He et al. / Powder Technology 313 (2017) 332–343

$$F(\phi, \mathrm{Re}_m) = \frac{F_{\mathrm{isol}}(\mathrm{Re}_m)}{(1-\phi)^3} + F_\phi(\phi) + F_{\phi,Re_m}(\phi, \mathrm{Re}_m)$$

$$F_\phi(\phi) = \frac{5.81\phi}{(1-\phi)^3} + 0.48\frac{\phi^{1/3}}{(1-\phi)^4}$$

$$F_{\phi,\mathrm{Re}_m}(\phi, \mathrm{Re}_m) = \phi^3\,\mathrm{Re}_m\left(0.95 + \frac{0.61\phi^3}{(1-\phi)^2}\right).$$

Normalized mean drag force from current simulation compare to F&H, T&H and T&Z correlation.

Re	Φ	IBM	F&H	% diff	T&H	% diff	T&Z	% diff
10	10%	3.58	2.78	−22.51%	3.65	1.99%	3.49	−2.72%
50		5.82	5.66	−2.80%	6.26	7.47%	5.92	1.67%
100		8.46	8.76	−3.58%	9.14	8.14%	8.29	−1.96%
200		14.10	14.45	2.53%	14.60	3.61%	12.32	−12.62%
10	20%	6.87	4.39	−35.10%	6.57	−4.34%	6.30	−8.37%
50		11.13	8.95	−19.66%	10.43	−6.28%	9.88	−11.29%
100		15.81	13.66	−13.57%	14.74	−6.75%	13.41	−15.16%
200		24.97	22.02	−11.78%	22.89	−8.30%	19.47	−22.01%
10	30%	13.14	7.46	−43.18%	11.98	−8.81%	11.57	−11.89%
50		20.20	15.38	−23.83%	18.38	−9.02%	17.56	−13.06%
100		27.58	23.29	−15.56%	25.59	−7.21%	23.63	−14.31%
200		42.82	36.77	−14.11%	39.34	−8.13%	34.27	−19.97%
10	35%	19.38	10.85	−44.01%	16.41	−15.32%	15.99	−17.46%
50		26.83	21.42	−20.16%	25.02	−6.75%	24.20	−9.83%
100		36.59	34.39	−6.01%	34.81	−4.86%	32.66	−10.75%
200		57.76	60.34	4.46%	53.52	−7.34%	47.64	−17.53%

$$c_D = \frac{8}{\mathrm{Re}}\frac{1}{\sqrt{\Phi_\parallel}} + \frac{16}{\mathrm{Re}}\frac{1}{\sqrt{\Phi}} + \frac{3}{\sqrt{\mathrm{Re}}}\frac{1}{\Phi^{\frac{3}{4}}} + 0.42\,10^{0.4(-\log\Phi)^{0.2}}\frac{1}{\Phi_\perp}$$

Human Learning versus Machine Learning

Human Learning

Sphere (Stokes flow): $c_D = \frac{24}{Re}$

add non-spherical shape

Non-spherical particle (Stokes flow):

$$c_D = \frac{8}{\mathrm{Re}} \frac{1}{\sqrt{\Phi_\perp}} + \frac{16}{\mathrm{Re}} \frac{1}{\sqrt{\Phi}}$$

D. Leith, Aerosol Sci. Tech. 6 (1987) 153

add large Re

Non-spherical particle ($Re < 10^5$):

$$F_{\text{isol}}\left(\mathrm{Re}_m\right)$$

add concentration

$$F(\phi, \mathrm{Re}_m) = \frac{F_{\text{isol}}\left(\mathrm{Re}_m\right)}{(1-\phi)^3} + F_\phi(\phi) + F_{\phi,Re_m}(\phi, \mathrm{Re}_m)$$

Machine Learning

$$\boldsymbol{F}_i = \langle \boldsymbol{F}_i \rangle (Re, \phi) + \Delta \boldsymbol{F}_i (Re, \phi, \{\boldsymbol{r}_{j=1}, \ldots, \boldsymbol{r}_{j=M}\}),$$
$$\boldsymbol{T}_i = \Delta \boldsymbol{T}_i (Re, \phi, \{\boldsymbol{r}_{j=1}, \ldots, \boldsymbol{r}_{j=M}\}),$$

Seyed-Ahmadi and Wachs (2020)

Neighbor configuration

input features for ANN

$$[\, Re, \phi, x_1, y_1, z_1, x_2, y_2, z_2 \ldots x_n, y_n, z_n]$$

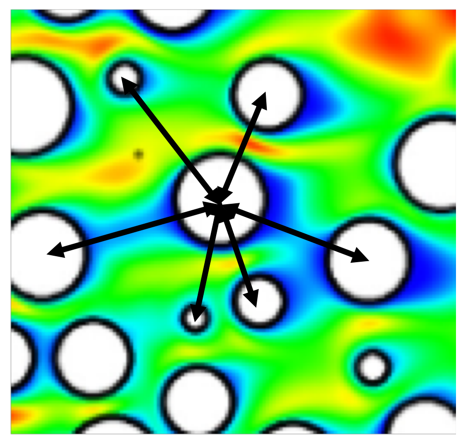

He and Tafti 2019

Still spherical particles

Problems

Curse of dimensionality:
As the number of features or dimensions grows, the amount of data we need to generate grows exponentially.

1 neighbor   Input: $\boldsymbol{r}_j = (x_j, y_j, z_j)$ Output: F_d, c_d $D_1 = 3, \quad N_1 = 1000$

15 neighbor   Input: $15 \times 3 = 45$ Output: F_d, c_d $D_2 = 45, \; N_2 = N_1^{D_2/D_1} = 1000^{15}$

Table 1
Number of spherical particles tested at each solid fraction.

Number of particles (N)	$\phi = \mathbf{0.1}$	191
	$\phi = \mathbf{0.2}$	382
	$\phi = \mathbf{0.3}$	573
	$\phi = \mathbf{0.35}$	669

each particle are collected, to yield 21,780 data points. All forces are further normalized using the Stokes-Einstein relation:

The input is a vector containing 47 features (1 Reynolds number, 1 solid fraction, relative distance in(x,y,z) from the nearest 15 neighboring particles).

Overfitting

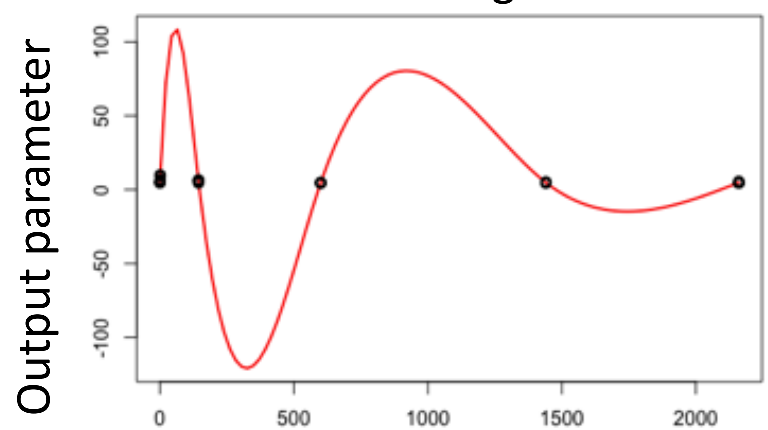

Input parameter

He and Tafti 2019

1. Reduce the number of dimensions
2. Increase the sample size

Introduce our team and methodology

Subteam 1: Experiment

Rui Ni

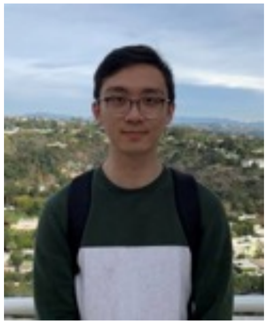

Xu Xu

Subteam 2: Simulation

Gretar Tryggvason

Jiacai Lu

Diagnostic methods

Drop tower (Re, Φ)

Dimension reduction

Particle-resolved DNS

Validation

Training

TensorFlow

MFiX

Training

Validation

Using Machine Learning for closure terms in multiphase flow modeling

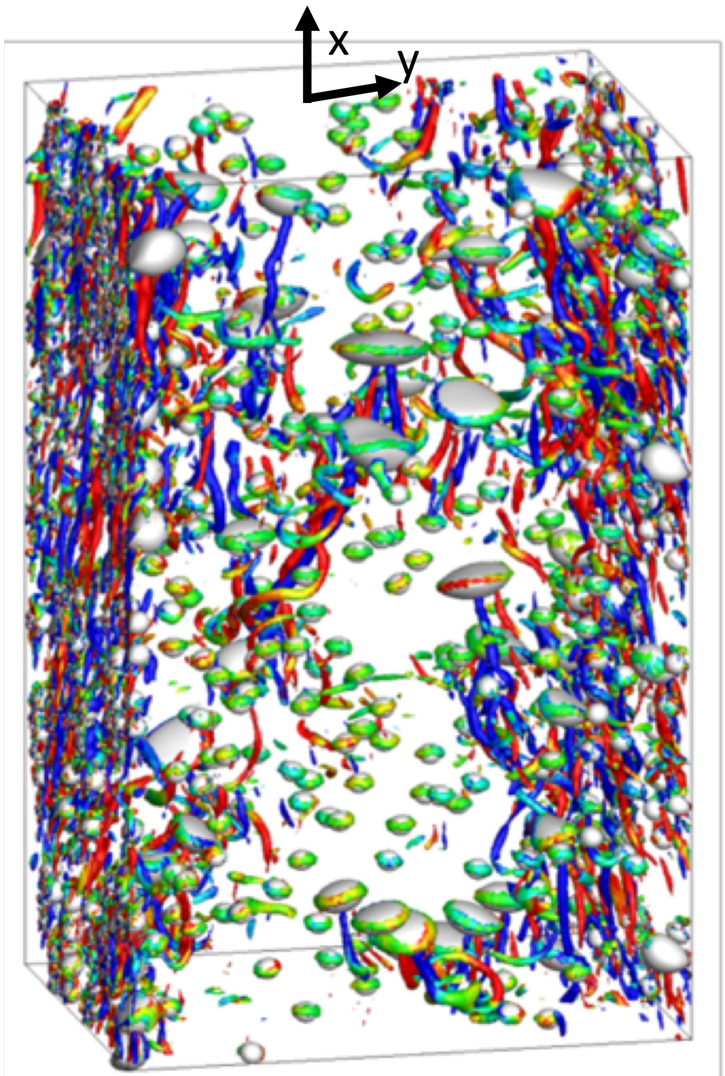

For turbulent flow, the fluxes depend both on resolved variables like void fraction and vertical velocity and on variables describing the average state of the unresolved state.

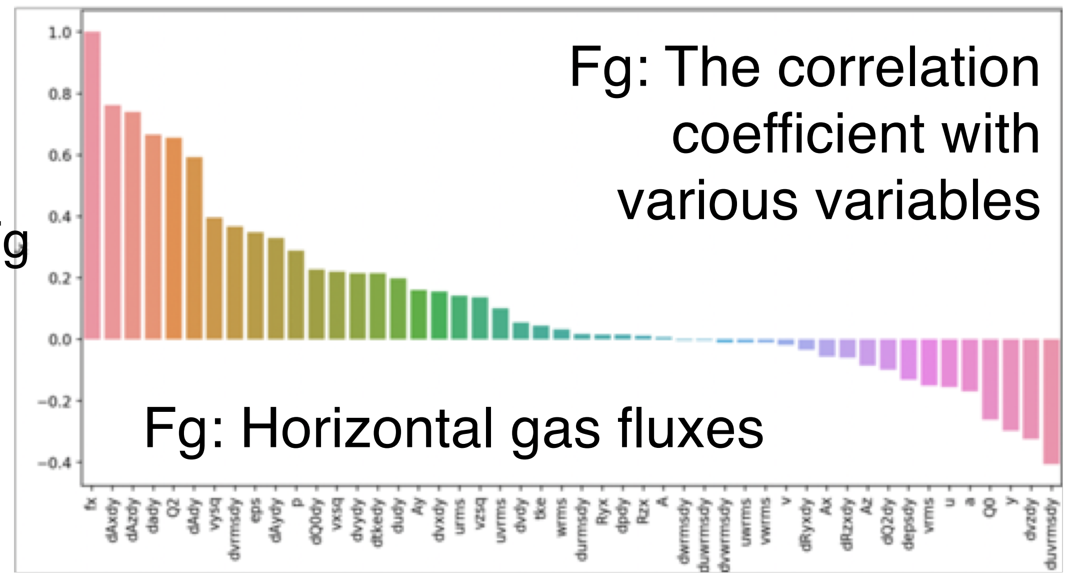

Using Machine Learning for closure terms in multiphase flow modeling

Fg: The importance of various features as measured by the Gini coefficient

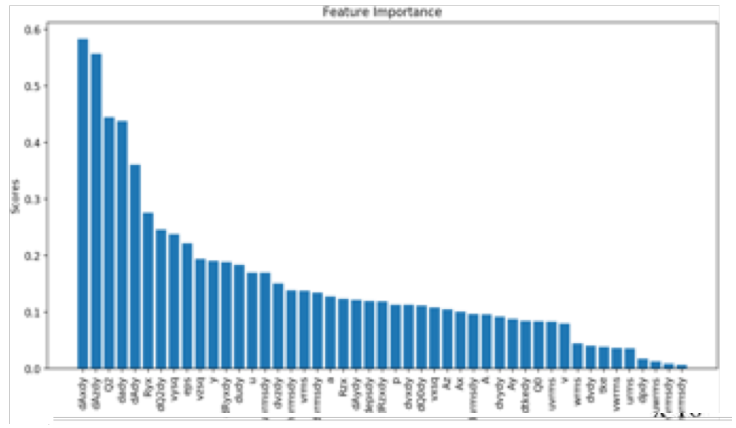

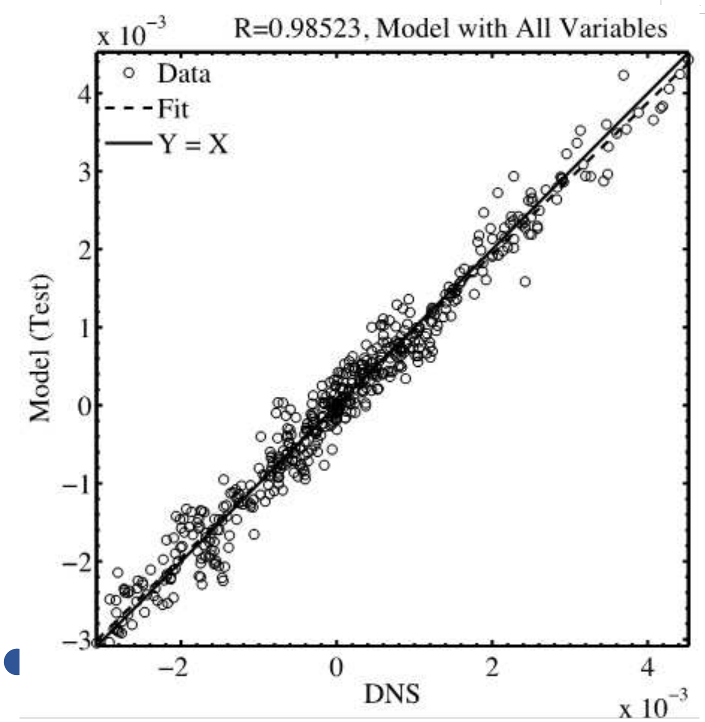

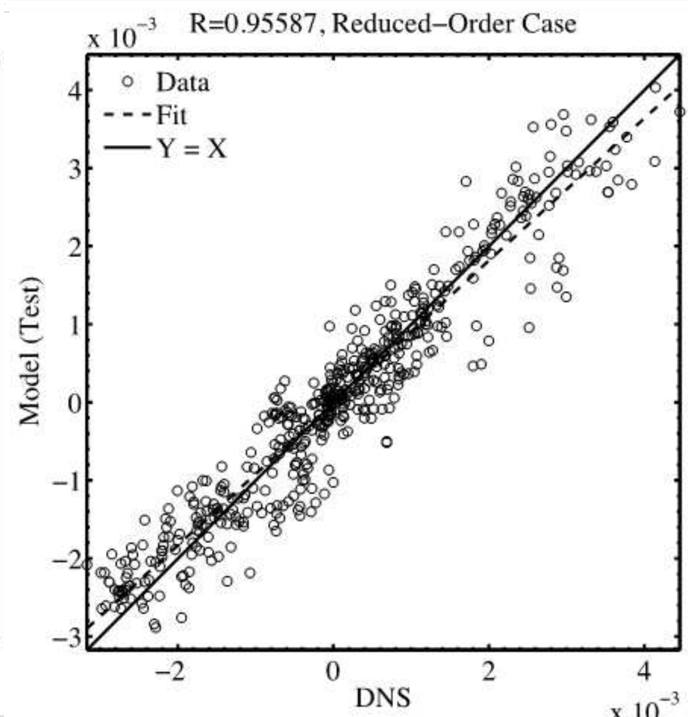

Flow around a falling solid sphere

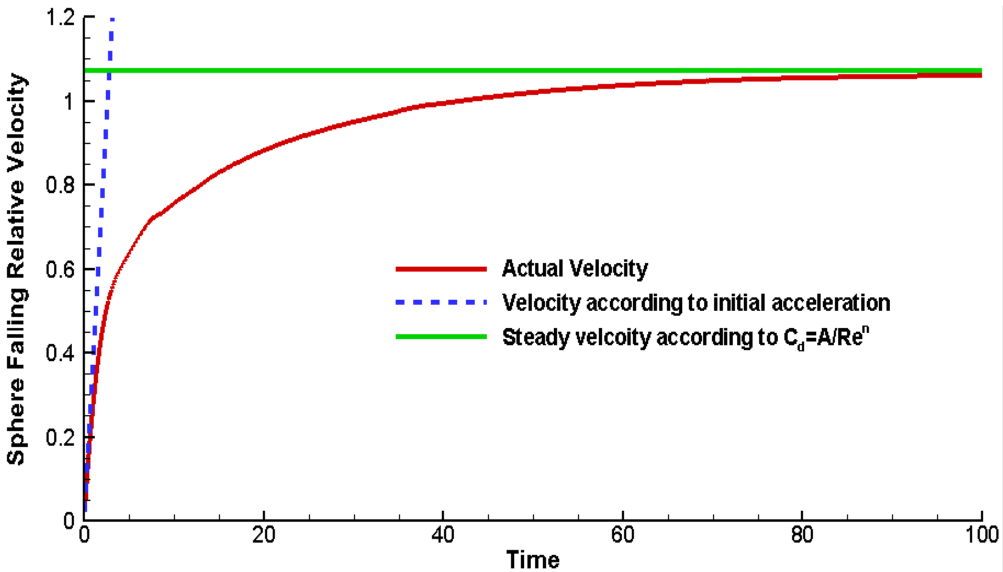

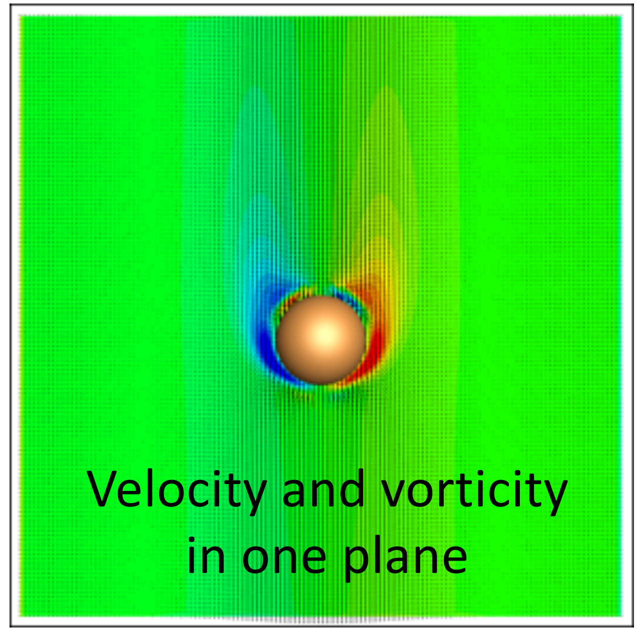

Solid motion is computed by solving the fluid equations for the whole domain, with the correct density in the solid and the fluid.

A solid body motion is imposed in the solid by correcting the velocity in an iterative manner.

Collision is accounted for by adding repulsion forces. Proximity is determined using index functions on the grid used for the solving the fluid equations.

Falling solid spheres

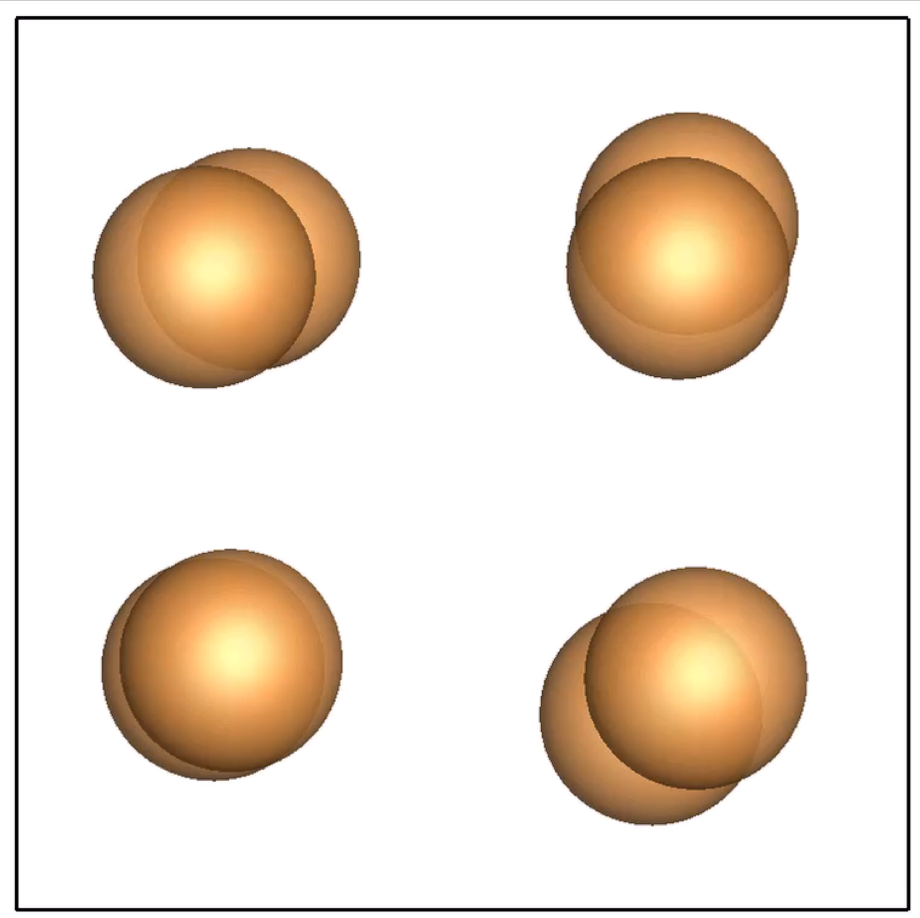

The unsteady motion of 8 spheres in a periodic domain, viewed from above

The trajectories of the centroids of spheres in a periodic domain viewed from above. The circles denote the initial conditions. Trajectories leave and enter the domain

Falling solid spheres

The Reynolds number of 8 solid spheres falling in a periodic domain versus time

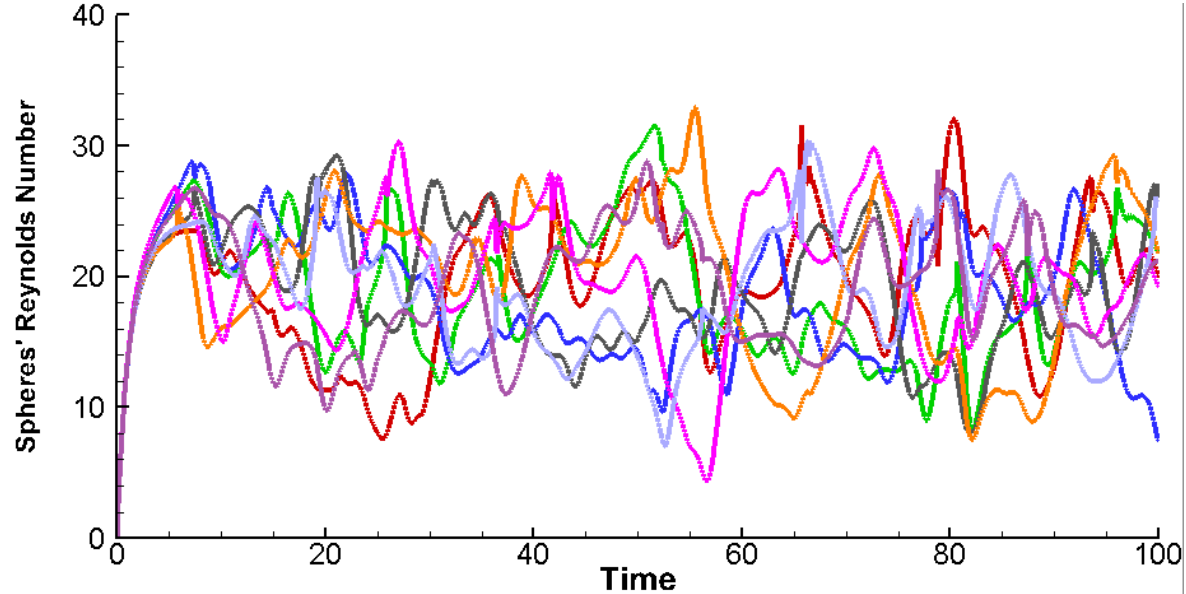

The instantaneous drag coefficient of each sphere versus time, computed from the slip velocity and the acceleration of each sphere

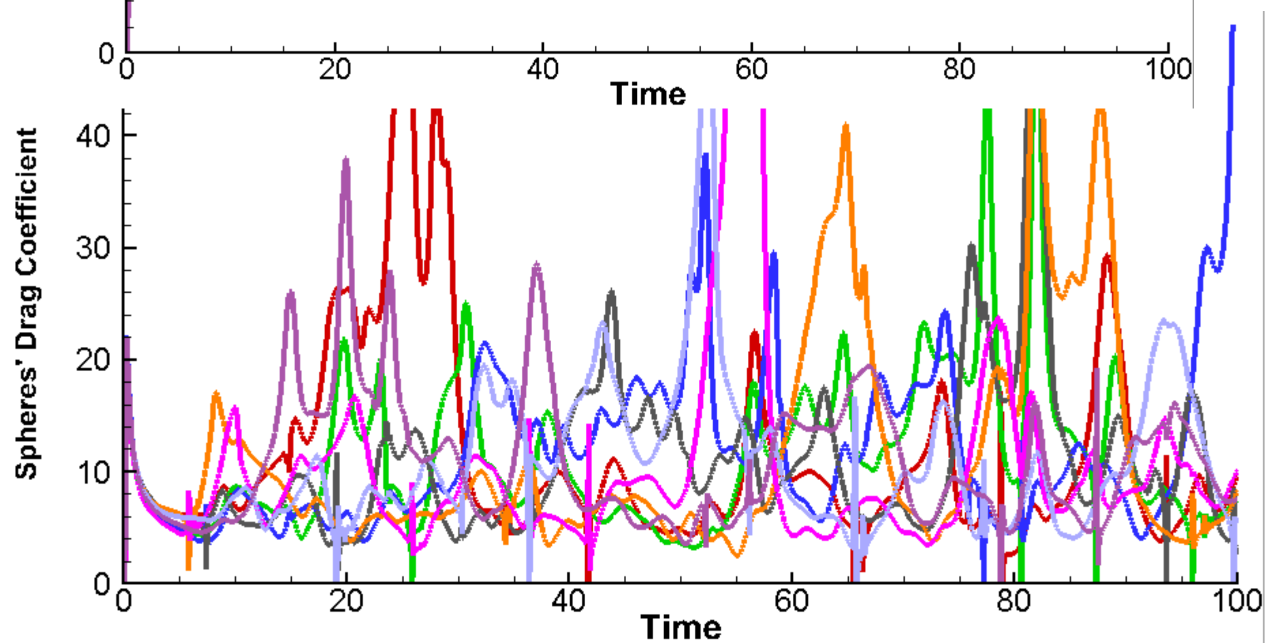

Falling solid ellipsoids

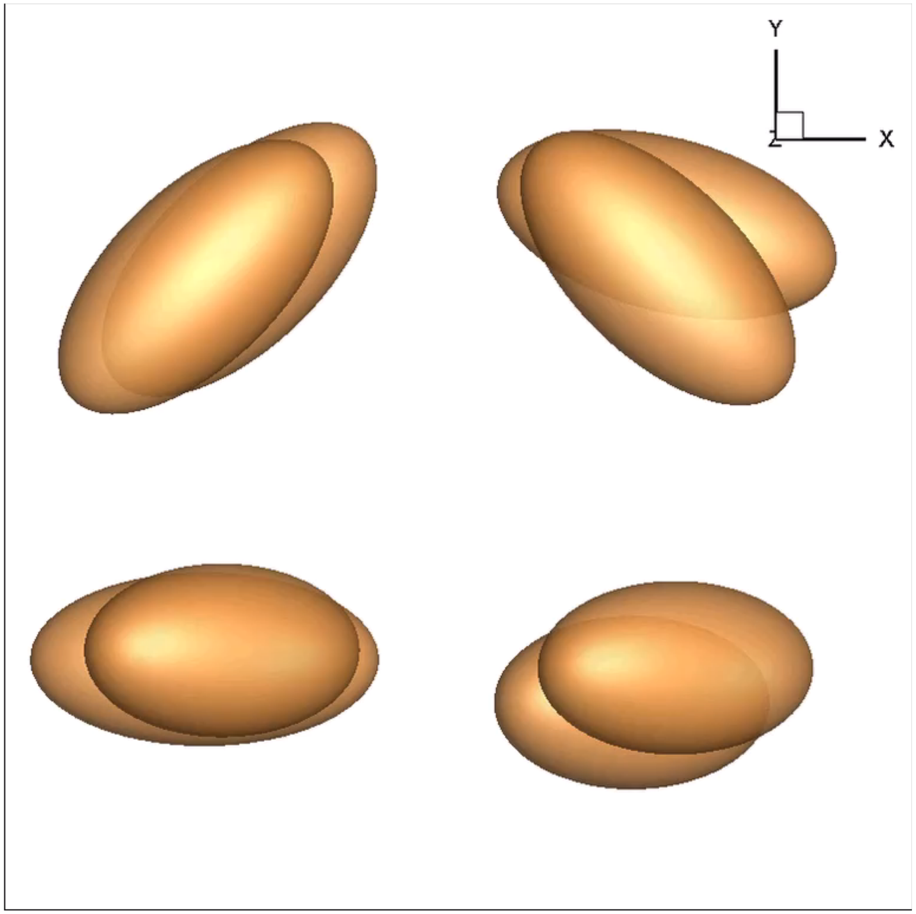

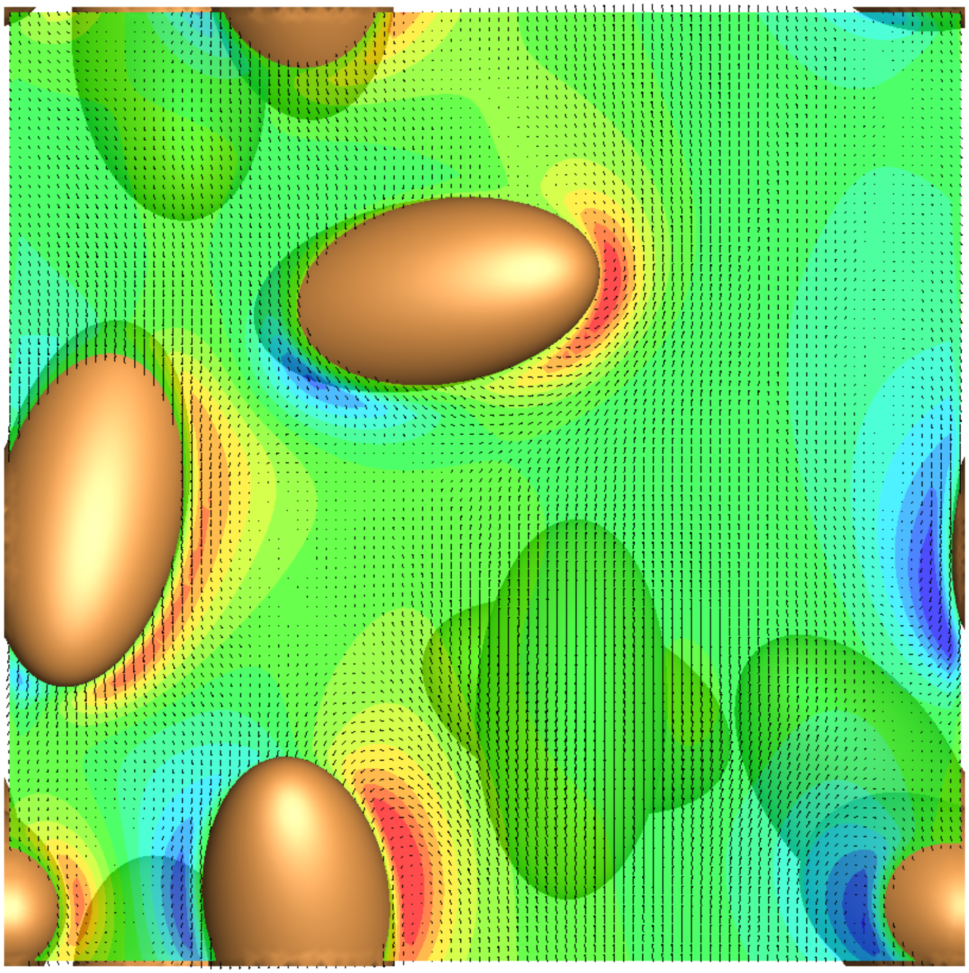

The unsteady motion of 8 ellipsoids in a periodic domain, viewed from above

The 8 ellipsoids and the velocity and vorticity field in one plane, viewed from the side

Falling solid ellipsoids

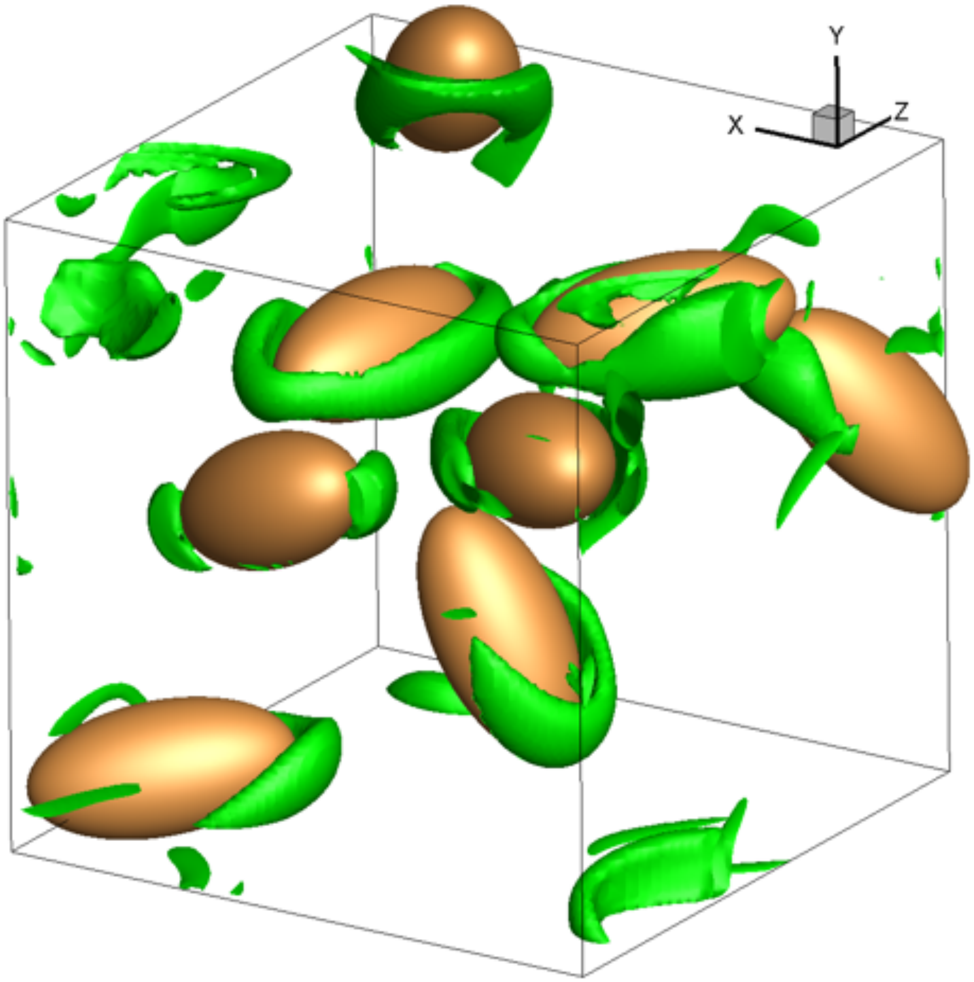

The vorticity around falling ellipsoids. The vortices is identified by the iso-surface of $\lambda_2 = -2.0$

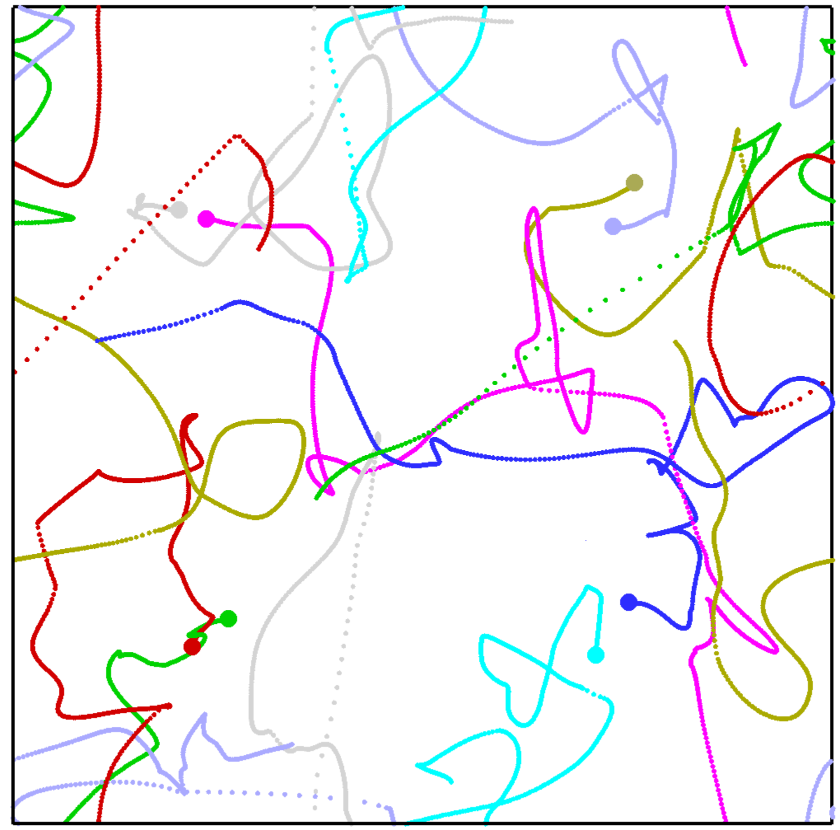

The trajectories of the centroids of the ellipsoids in a periodic domain viewed from above. The circles denote the initial conditions. Trajectories leave and enter the domain constantly.

Experiments

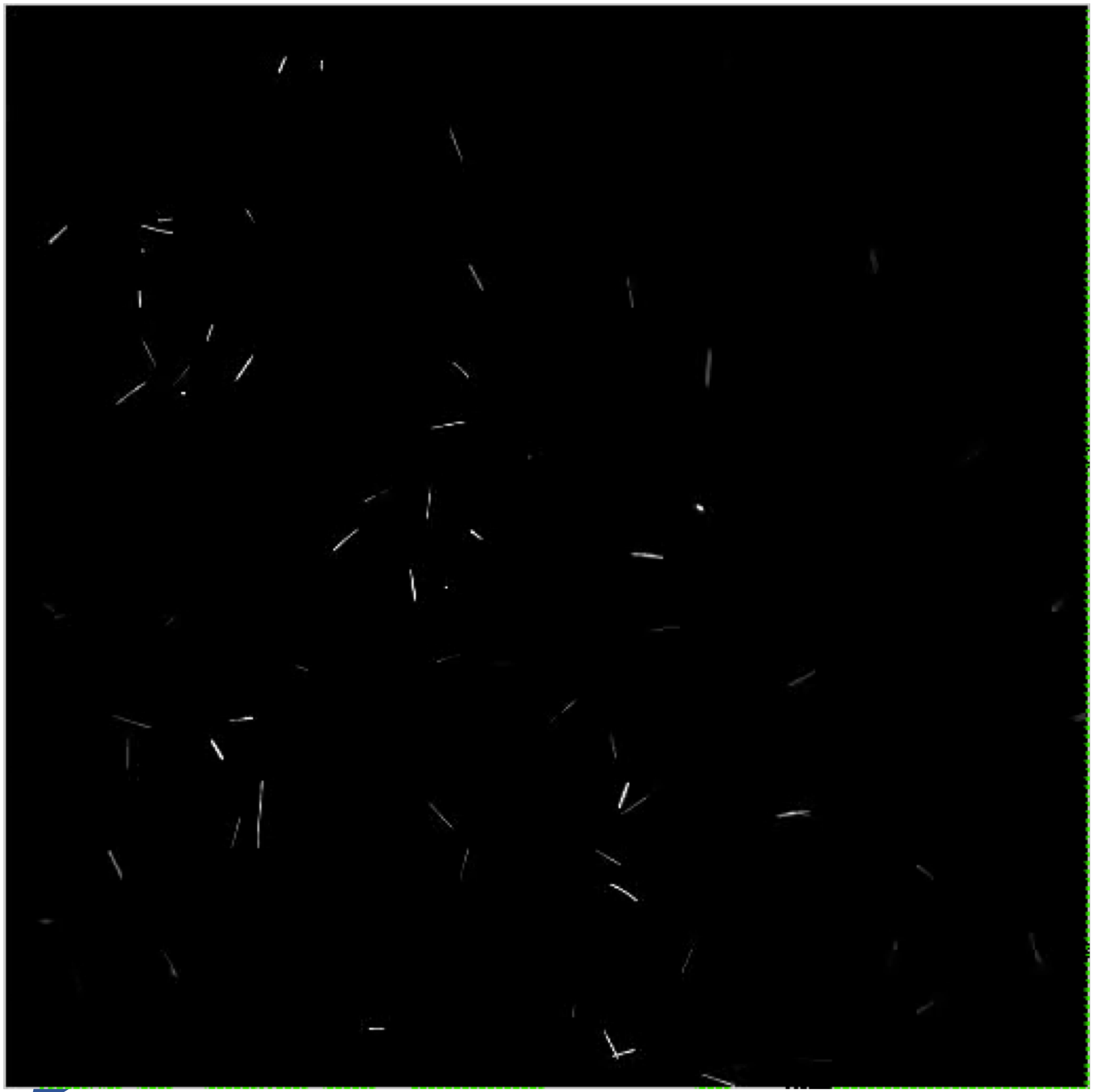

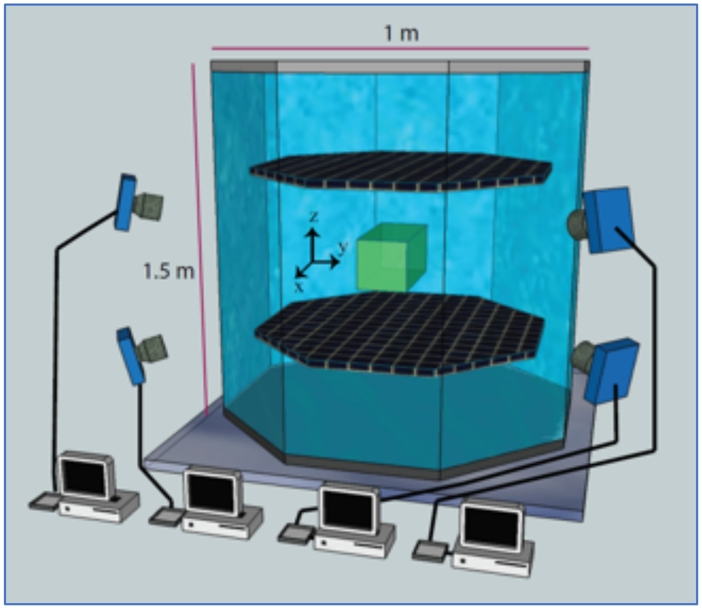

$700 \times 30 \times 30\ \mu m$

- Turbulent flow
  - 1m x 1m x 1.5m plexiglas tank
  - Two oscillating grids (in phase)
  - Grid mesh size = 8cm

Pair orientation

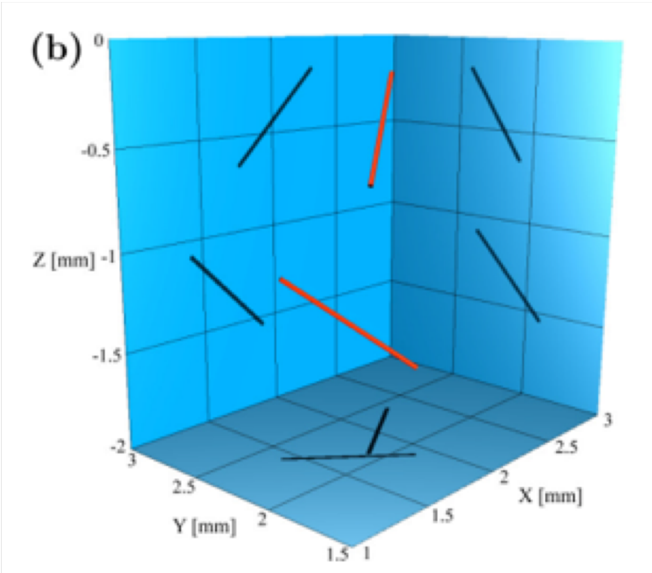

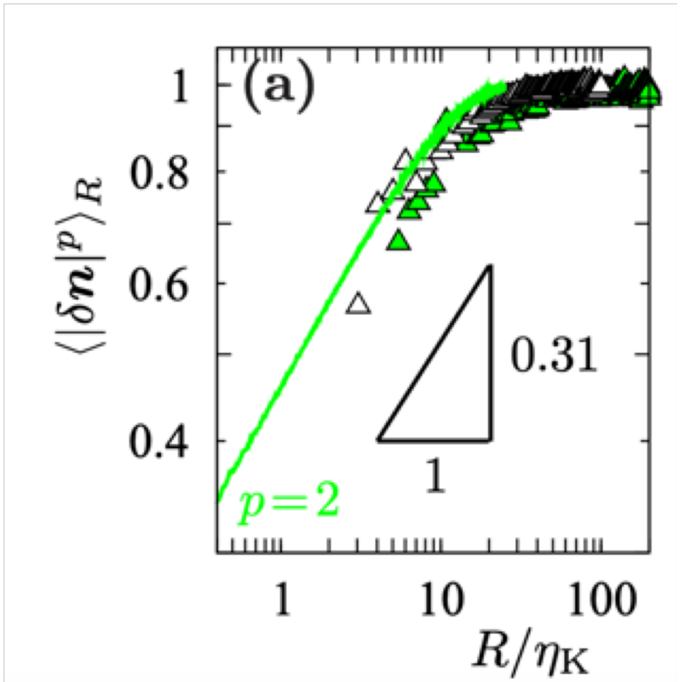

Extracting particle orientations and positions by using multiple cameras.

$$\frac{d}{dt}\boldsymbol{n} = \mathbb{O}\boldsymbol{n} + \Lambda\mathbb{S}\boldsymbol{n} - \Lambda(\boldsymbol{n}\cdot\mathbb{S}\boldsymbol{n})\boldsymbol{n}$$

Experiments

Cyclone separator

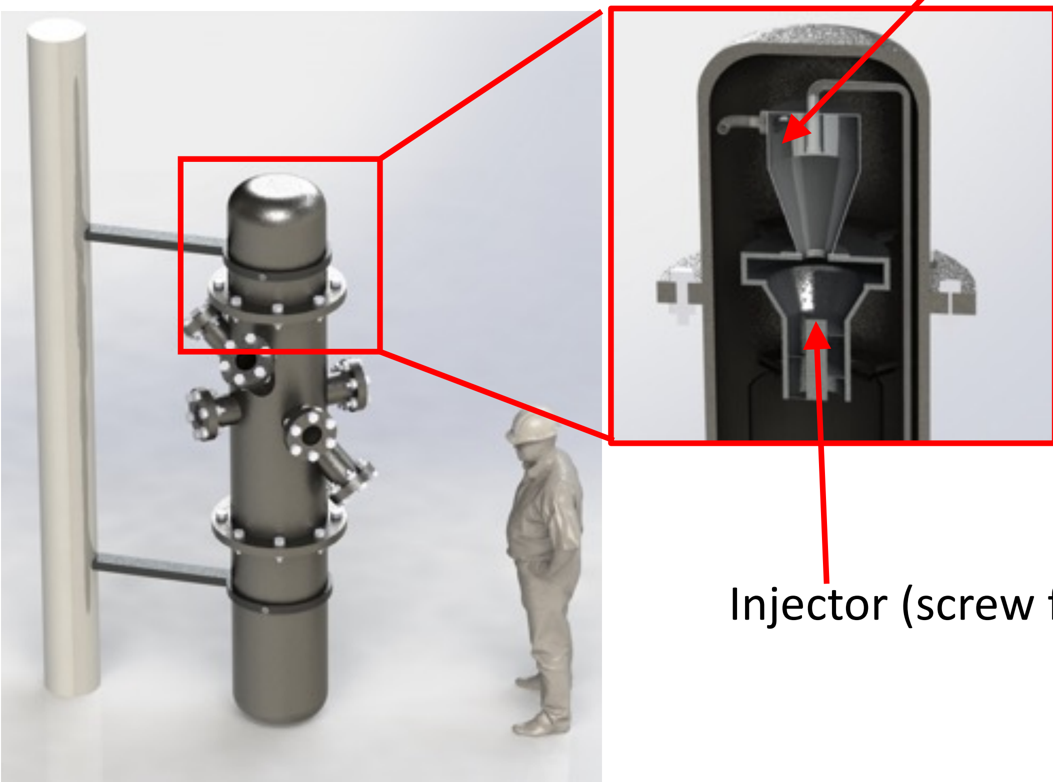

Injector (screw feeder)

Drop tower

Plan

Subteam 1: Experiment

Rui Ni

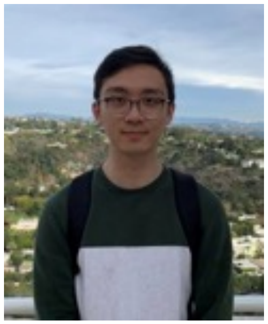

Xu Xu

Subteam 2: Simulation

Gretar Tryggvason

Jiacai Lu